Anal Bioanal Chem (2009) 395:1693–1706
DOI 10.1007/s00216-009-3052-x

ORIGINAL PAPER

Electrodeposition polymers as immobilization matrices in amperometric biosensors: improved polymer synthesis and biosensor fabrication

Dmitrii A. Guschin · Halyna Shkil · Wolfgang Schuhmann

Received: 14 May 2009 / Revised: 13 July 2009 / Accepted: 10 August 2009 / Published online: 10 September 2009

Abstract Electrodeposition polymers can be precipitated on electrode surfaces upon electrochemical-induced modulations of the pH value in the diffusion zone in front of the electrode. The formed polymer films can be used as immobilization matrices in amperometric biosensors. In order to rationally control the thus obtained biosensor properties, it is indispensable to develop strategies for the reproducible synthesis of electrodeposition polymers as well as methods for the non-manual and reproducible sensor fabrication. Based on instrumental developments such as a specifically designed parallel synthesizer with improved stirring and temperature control, an automatic pipetting robot for the preparation of the monomer mixtures and controlled removal of polymerization inhibitors, the reproducible synthesis of libraries of electrodeposition polymers was achieved. Moreover, the polymerization process could be monitored using in-line thermocouples, and it could be shown that the chosen strategies led to reproducible polymerization reactions. By adaptation of an electrochemical robotic system integrating a Au microtiter plate and automatic electrode cleaning by means of a polishing wheel reproducible biosensor fabrication using glucose oxidase as a model enzyme could be demonstrated. These results open the route for the rational development of biosensors and control of the sensor properties by choosing specifically designed electrodeposition polymers.

Keywords Copolymerization · Electrodeposition paints · Reproducibility · Parallel synthesis · Biosensor

D. A. Guschin · H. Shkil · W. Schuhmann (✉)
Analytische Chemie—Elektroanalytik & Sensorik,
Ruhr-Universität Bochum,
Universitätstr. 150,
44780 Bochum, Germany
e-mail: wolfgang.schuhmann@rub.de

Introduction

Amperometric enzyme electrodes and especially glucose oxidase-based biosensors had been described extensively during the almost 50 past years, and there are far more than 5,000 publications related to these types of biosensors. However, in most cases, the immobilization procedure used for the fabrication of the biosensors was manual and was not exclusively addressing the electrode surface. Most simply, immobilization was performed manually by drop or dip coating of liquid enzyme preparations containing suitable crosslinkers [1] or precursors for the formation of sol–gel matrices [2, 3]. However, non-manual procedures were assumed to offer better reproducibility and better control of the immobilization process, which is crucial particularly when aiming at miniaturized devices and selectively immobilizing the recognition elements on single electrodes out of a microelectrode array. A number of non-manual immobilization protocols have been described, which include screen-printing techniques [4] together with photo-induced crosslinking [5], spin-coating procedures followed by photolithographic structuring and lift-off [6], and dispensing polymer/enzyme mixtures using ink-jet printers or piezo-actuated microdispensers [7]. In addition, electrochemical techniques were intensively applied to address the surface of an electrode as immobilization site. Electrochemically induced formation of biomolecule-containing polymer films by means of electrophoretic accumulation [8, 9] and deposition of conducting polymers [10–13] such as polypyrrole, polyaniline, and polythiophene were successfully used. Additionally, conducting polymers were modified with suitable redox relays in order to improve the electron-transfer characteristics between the polymer-integrated biological recognition element and the electrode surface [14, 15]. However, as a major drawback,

it became clear that conducting polymers are deposited via intermediate, highly reactive radical cations implying a strict exclusion of molecular oxygen, and hence resulting in a rather complicated sensor production process.

Recently, we introduced electrodeposition polymers as an alternative electrochemical approach for the non-manual immobilization of active biosensor elements on electrodes surfaces. The use of electrodeposition polymers avoids the formation of highly reactive intermediate species, and immobilization of biorecognition elements is based on polymer entrapment during electrochemically induced modulation of the polymer solubility [16, 17]. Electrodeposition polymers are suspensions of polyelectrolyte particles in aqueous medium stabilized electrostatically by the charge on the polymer particles. During an electrochemically induced pH-value modulation in the diffusion zone in front of the electrode surface—invoked either by water oxidation or water reduction—the charges at the polymer backbone are neutralized leading to flocculation and enlargement of the particles followed by precipitation on the electrode surface [18, 19]. During the formation of the polymer film caused by pH-induced precipitation of the electrodeposition polymer, any high-molecular weight biorecognition element, which is present in the electrolyte in front of the electrode surface, is simultaneously entrapped and co-deposited within the copolymer film [16, 17, 20]. The resulting polymer film is swelling in aqueous solution under formation of a hydrogel, thus allowing fast diffusional mass transport of the substrate to the site of the immobilized biological element. Moreover, hydrogels are known to stabilize integrated proteins, thus leading to an improved operation stability of the biosensor.

Since we have introduced electrodeposition polymers as immobilization matrix in amperometric biosensors [16], several groups have used predominantly commercial electrodeposition polymers for the fabrication of bioanalytical devices [21–23]. However, commercial electrodeposition polymers are usually optimized for other applications such as corrosion protection, and the additives may not be beneficial for the entrapped biological recognition elements. Moreover, they do not offer suitable functional groups for the integration of additional components, which may be essential for the proper function of a sensor such as redox relays for the design of reagentless biosensors. Thus, the development of libraries of specifically synthesized electrodeposition polymers is important for understanding of the properties of immobilization matrices and their impact on the sensor properties. Previously, we have described initial steps for the synthesis of libraries of electrodeposition polymers using bulk or emulsion polymerization initiated by radical starters [24]. Initial ideas of how the specific monomer properties are influencing the polymer characteristics and their impact on the biosensor responses were derived.

To further evaluate the future possibilities of electrodeposition polymers for biosensor design and fabrication, it is indispensable to improve the understanding of the polymer formation process and to improve the reproducibility of the polymer synthesis and the sensor fabrication. Based on these prerequisites, an in-depth understanding of the complex interplay of the parameters, which determine the biosensor properties, has to be achieved. Therefore, in this communication, strategies for the improved and reproducible synthesis of electrodeposition polymers as well as automated and hence reproducible biosensor fabrication processes are demonstrated.

Results and discussion

For the optimization of electrodeposition paints with respect to their properties as immobilization matrix for amperometric biosensors, two main prerequisites have to be kept in mind. On the one hand, it is indispensable to control the polymer synthesis process to an as large as possible extent to assure high reproducibility of the polymer properties, which are in a complex way determining the properties of the derived biosensors. On the other hand, the sensor fabrication process itself has to be highly reproducible to allow for a comparison and hence optimization of different electrodeposition polymers. In principle, two options are seen, namely the utilization of commercial electrodeposition paints, which are produced at industrial scale with high reproducibility or the careful evaluation of synthetic routes for the design of specifically adapted electrodeposition polymers.

As a matter of fact, the synthesis of electrodeposition polymers for optimizing their properties in accordance with the specific functions of derived amperometric biosensors is the only possible option if specific molecular architectures on electrode surfaces are envisaged. The synthesis of electrodeposition polymers provides the basis for the design of immobilization matrices with adapted properties with respect of influencing parameters such as hydrophilicity/hydrophobicity ratio, diffusional mass transport of substrate and product of the enzymatic reaction within the polymer film, local pH value, potential stabilization of polymer-entrapped biological recognition elements, and even more important, the functionalization of the polymer backbone with specific functional groups for later crosslinking or binding of, e.g., redox mediators.

In our initial attempts to investigate libraries of electrodeposition paints [20, 24], we assumed that a radical emulsion polymerization at controlled temperature initiated by a radical starter will lead to a statistical distribution of all

monomers within the polymer backbone. These investigations unequivocally proved the large variations of the polymer properties and their impact on the biosensor properties. For the synthesis of an electrodeposition polymer, a balance between pH-dependent side chains and hydrophobic side chains has to be found, which is predefining the solubility of the polymer in aqueous solution. If the polymer backbone is too hydrophilic, pH modulation will not lead to a precipitation of the polymer. In contrast, if the polymer backbone is too hydrophobic and the number of pH sensitive side chains is small, the polymer cannot be dissolved in water at all. In order to investigate the reproducibility of the synthesis procedure, an emulsion polymerization was repeated four times with exactly the same monomer composition used as a starting set taken from our previous knowledge about the influence of the polymer side chains on the final polymer properties (4.5% butyl acrylate, 36.7% dimethylaminoethyl methacrylate, 4.5% methyl methacrylate, 22.3% cyclohexyl methacrylate, and 32.5% 1-imidazolyl-hex-5-en-3-oxy-2-ol) while controlling as far as possible the parameters during the radical-initiated emulsion polymerization. The obtained polymers were then used for the fabrication of glucose biosensors by entrapping glucose oxidase during an electrochemical-induced pH modulation causing precipitation of the polymers. Glucose calibration graphs were obtained by means of chronoamperometry and oxidation of enzymatically formed H_2O_2 at the underlying platinized graphite electrode surface (Fig. 1).

As can be clearly seen, the variation in the sensor response obtained from the four polymer preparations is large, suggesting either a significant irreproducibility of the polymer formation process or of the biosensor fabrication by means of electrochemically induced pH modulation.

In order to evaluate the source of irreproducibility, the obtained polymers were investigated by means of ^{1}H NMR spectroscopy (Fig. 2), which was only possible after the introduction of an imidazolyl- or pyridyl-functionalized monomer in the polymerization mixture. After an initial NMR spectrum, in which the characteristic signals of the imidazole ring are clearly seen at 7.5–8.0 ppm, was recorded from the reaction mixture, the electrodeposition polymer was precipitated by increasing the pH value. A second NMR spectrum from the precipitated fraction did not show any signals of the imidazole substituent.

During the radical-initiated polymerization, the imidazolyle-functionalized monomer is obviously not included into the polymer backbone. There is an extensive literature on theoretical, experimental, and applied aspects of copolymerization reactions, including early work on kinetic models [25, 26]. From these investigations, it is obvious that the overall composition of the resulting copolymer depends on the reactivity ratios, initial monomers mixture composition, and overall yield of the polymerization reaction. The composition of the monomer mixture changes during the course of the polymerization if one of the monomers is preferentially incorporated into the copolymer backbone.

Taking this into account, it was attempted to balance the drift in the copolymer composition by adjusting the initial ratios of the monomers in the reaction mixture. However, this was not successful since the increase of the relative amount of less active monomers directly affected the overall polymerization yield and hence again the polymer composition. The reactivity ratio of the monomers depends on both the nature of the monomers itself and the reaction conditions for the radical-initiated emulsion polymerization. Thus, the obvious possibility to minimize the drift in the polymer composition is either seen in optimizing the polymerization conditions or by selecting monomers with similar reactivity. By changing the reactions conditions during the polymerization reaction, the overall conversion yield can be varied, which will influence the relative composition of the monomers in the polymer backbone. However, a study of the polymerization process suggests a weak dependence of the reaction temperature and the duration of the heating on the resulting polymer composition. These findings are in accordance with previous reports

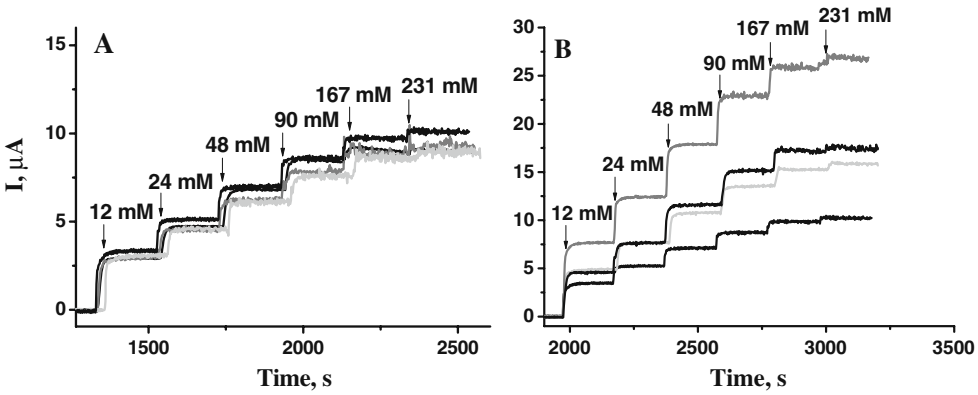

Fig. 1 Chronoamperometric calibration (**a**) of four glucose sensors fabricated using the same polymer and (**b**) of four biosensors using four polymers, which had been synthesized according to the same synthesis protocol using the same initial mixture of the monomers and conditions for the emulsion polymerization

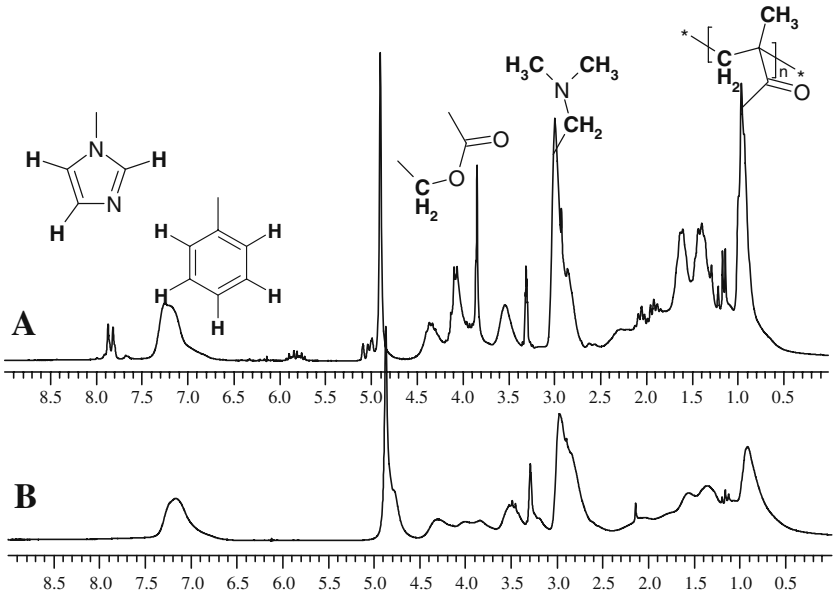

Fig. 2 ^{1}H NMR spectra in d_4-MeOH of the solid content of the EDP Cp7 before (**a**) and after (**b**) precipitation

and are due to the fact that the effect of temperature on the reactivity ratio of the monomers is insignificant since activation energies for radical propagation are relatively small [27].

To further evaluate the shift in the monomer composition, the effect of different polymerization techniques was evaluated. Emulsion polymerization for the preparation of cathodic electrodeposition polymers was carried out in the absence of any detergent, and the formed polymer suspension was stabilized by electrostatic repulsion between the protonated dimethylamino groups at the surface of the formed particles [19]. For comparison, polymerization reactions were carried out in emulsion, bulk, or solution using methanol as solvent without addition of any acid. By this, the polarity of the initial monomer mixture was varied. Table 1 shows the influence of the polymerization conditions on the relative amount of monomers within the formed polymers as calculated from the ^{1}H NMR spectra.

Table 1 Influence of the polymerization technique on the average composition and on overall conversion yield of the copolymers

Mol.%	Monomers mixture	Emulsion 1	Emulsion 2	Solution	Bulk
DMAEMA	33.3	56.8	26.2	41.0	33.1
BA	33.3	18.3	36.5	22.7	31.8
St	33.3	24.9	37.3	36.2	35.4
Conversion	0	69	70	46	76

"Emulsion 1" was carried out with neutralization of the basic monomers for electrostatic stabilization; "Emulsion 2", "Solution", and "Bulk" were carried out without any addition of acid

Obviously, in the case of the emulsion polymerization, the drift in monomer composition is maximal with respect to the monomer composition reflecting the fact that the monomer reactivity is affected especially at non-homogeneous conditions [28, 29]. This is most probably caused by the difference of the relative solubility of the different monomers in the formed particles and the dispersing medium or by the hindered diffusion of one or several monomers into the particles.

In the polymer formed by the emulsion polymerization after neutralization of the basic monomers (emulsion 1), dimethylaminoethyl methacrylate is predominantly enriched in the resulting copolymer. It is known that the monomer reactivity ratio for an acidic or basic monomer is dependent on the pH value [30, 31], which is confirmed by the high reactivity of protonated dimethylaminoethyl methacrylate, which could be polymerized at moderate temperatures (ca. 90 °C) in the absence of a radical initiator.

The observed polymer composition obtained in the solution polymerization confirms the importance of polarity effects of the medium. It becomes evident that copolymerization reactions involving combinations of polar and non-polar monomers are different depending on the polarity of the reaction medium [32]. On the other hand, the presence of a solvent or a dispersion medium leads to a comparatively low conversion yield during the polymerization reaction, which may be explained by a chain transfer to solvent.

As already pointed out above, the composition ratio in the resulting copolymers may be improved by using monomers of similar reactivity. It was shown previously that statistical copolymerization of the active acrylates with allyl [33] or olefin-based [34–36] monomers is difficult

most probably due to the different mechanisms through which the monomers undergo polymerization. Acrylates are readily polymerized through a free-radical mechanism, whereas allyl- and olefin-based monomers either undergo a slow free-radical polymerization or need quite harsh conditions. Moreover, polymerization of some acrylates can be affected by the presence of monomers such as allyl ethers [37].

Taking this into consideration, there are several possibilities for achieving a significant incorporation of a functionalized monomer within a copolymer backbone. One possibility is seen in the integration of an active acrylic precursor monomer such as acryloyl chloride, which may be later modified with the envisaged functionality.

In a first attempt, acryloyl chloride was copolymerized with butyl acrylate and dimethylaminoethyl methacrylate. The activated carboxy function was reacted with sodium imidazolate, and the obtained polymer was purified by precipitation with NaOH. The ^{1}H NMR data clearly confirmed the presence of imidazolyl groups in the obtained copolymer. However, a disadvantage is seen in possible side reactions of the highly activated carboxyl group with functional groups such as hydroxyl functions, which may be present at the monomers forming the electrodeposition polymer.

Alternatively, already functionalized (meth)acrylate monomers, which are in general not commercially available, were synthesized by reaction of the corresponding alcohols with methacryloyl chloride in the presence of a base as proposed previously [38, 39]. These reactions proceed with high yields (up to 90%), and the obtained products have to be stored in the presence of a polymerization inhibitor. The obtained functionalized monomers can be easily copolymerized with similar active (meth) acrylates. Figure 3 shows the ^{13}C NMR and ^{1}H NMR spectra of one of the obtained copolymers.

The monomers are quite similar, and therefore, many signals are overlapping in the corresponding NMR spectra. The signals from the imidazolyl group (120–140 ppm in ^{13}C or 8.0–7.5 ppm in ^{1}H) and from *N*-methyl group (42–50 and 3.2-2.5 ppm, correspondingly) are well separated from the other resonances, which confirm the presence of both monomers in the copolymer. Signals from methyl (17–21 ppm) and methylene (60–65 ppm) are very sensitive to compositional and stereochemical changes and can be used for evaluation of the microstructure of the copolymers.

In order to be able to modify at a later stage the obtained electrodeposition polymers, e.g., by coordinative binding of metal complexes, an extended library of acrylic-based monomers was established (Fig. 4). Due to the fact that

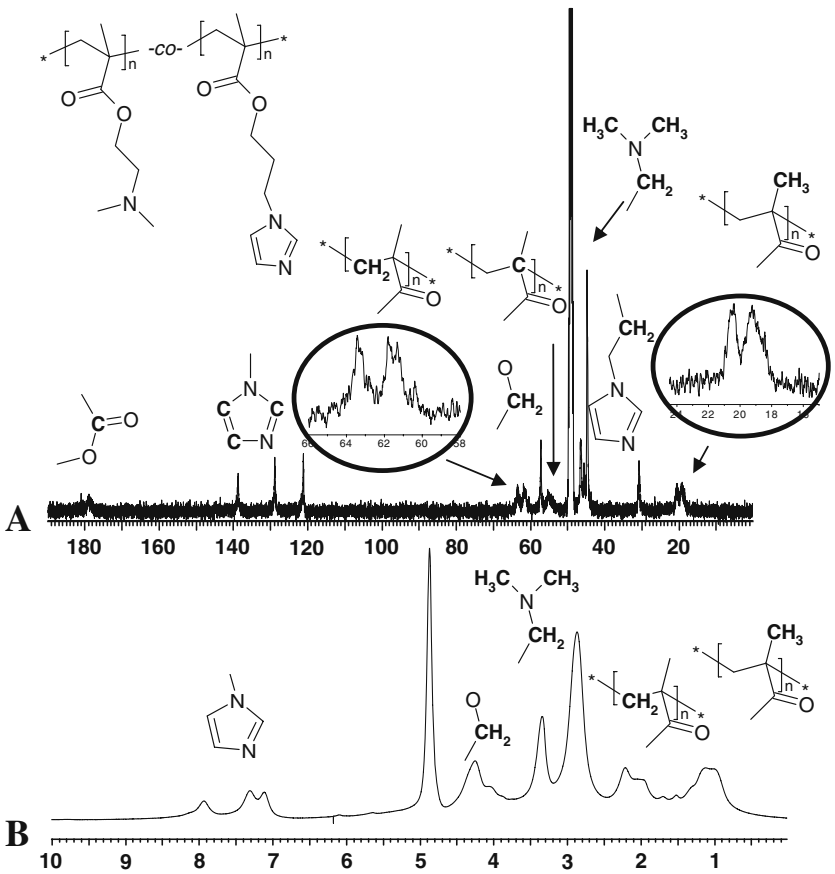

Fig. 3 ^{13}C NMR (**a**) and ^{1}H NMR (**b**) spectra in d_4-MeOH of the copolymer of ImPMA with DMAEMA

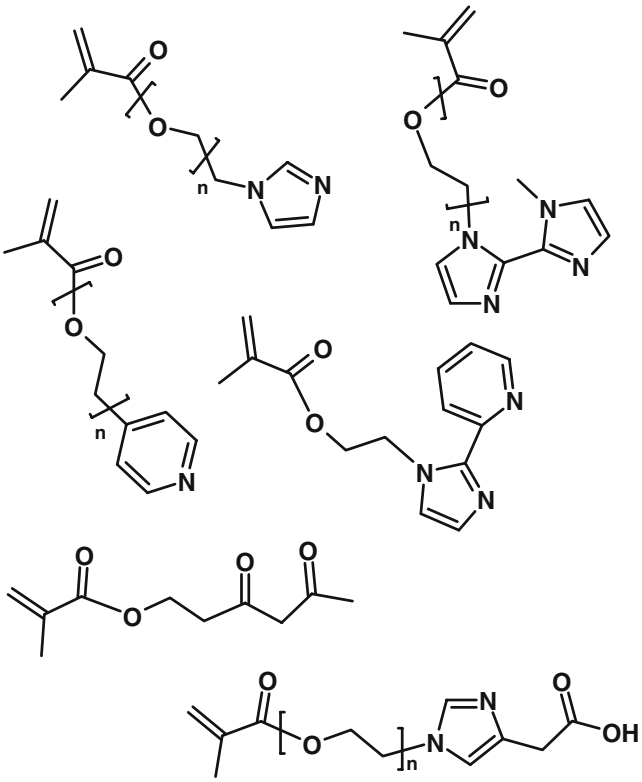

Fig. 4 Functionalized monomers with activated double bonds used for synthesis of electrodeposition paints

all these monomers are methacrylate derivatives, it can be assumed that the reactivity of these monomers is similar leading to their statistical integration into the polymer backbone during polymerization.

The reproducibility of the polymerization process and hence the reproducibility of the properties of the formed electrodeposition polymers depend on the one hand on the control of the polymerization process and on the other hand on variations of the experimental conditions. Especially, the possible variations of the experimental conditions can be addressed by designing adequate equipment. For this, the parallel polymerization setup, which had been used previously by us [20], was improved. First, the magnetic stirrer, which was only able to sufficiently stir the polymerization mixtures until a viscosity of about 1,000–1,500 cP, had to be replaced to accommodate all possible ranges of viscosity of the polymerizing mixture even to a viscosity range of 10^4 cP. Simultaneously, reproducibility of the heating of the reaction tubes had to be improved. Heating was previously achieved by a conventional hot plate equipped with a contact thermometer causing variations of up to 7 °C in different reactor tubes and temporary fluctuations in one reactor of about 8 °C. To overcome these experimental limitations, a parallel synthesizer was specifically developed, which enables stirring at high viscosity and a significantly improved temperature control together with an individual temperature measurement in each reaction tube by means of thermoelements. The setup is shown in Fig. 5.

The setup allows up to eight parallel polymerization reactions to be performed in 10-ml glass tubes equipped with reflux condenser, high-viscosity stirrer with integrated thermocouple for in-line temperature control. Heating is achieved with a high-precision heating plate in combination with a contact thermometer that allows to control the temperature of the heating bath with an accuracy of 0.2 °C. By means of a digital overhead stirrer with integrated viscosity control, a constant stirring speed with an accuracy of 10 rpm is achieved. The stirring speed can be monitored and controlled by means of a computer interface.

Temperature monitoring is achieved by means of a group of thermocouples connected to a data logger, which allows to record temperature variations within each individual reaction tube with an accuracy of 0.5 °C. By this, on-line monitoring of the polymerization rate becomes possible. Typical temperature profiles recorded during copolymerization reactions of different monomer compositions are shown in Fig. 6.

The temperature profiles can be used as a sensitive tool to monitor the course of the polymerization reactions. For comparison of different polymerization reactions on the one hand, the delay in polymerization which is dependent on the nature of the monomers, the presence of inhibiting compounds as well as the nature and amount of the radical initiator can be used. On the other hand, the maximal temperature during polymerization is mainly dependent on the composition of the monomer mixture. Hence, the recorded temperature profiles increase significantly the comparability of polymerization reactions and allow to investigate and optimize the influence of the purity of the

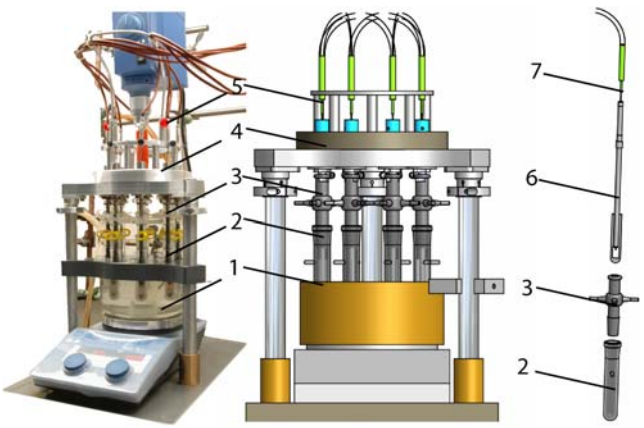

Fig. 5 Parallel polymerization reactor with improved stirring and temperature control. *1* Heating module, *2* reaction tube, *3* reflux condenser, *4* combined stirring module with rotational-speed sensor, *5* temperature monitoring module with individual thermocouples, *6* individual stirrer bar with integrated *7* thermocouple

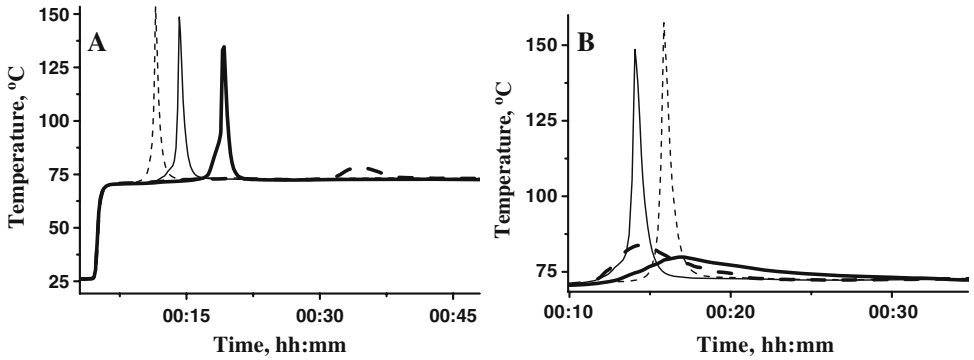

Fig. 6 Temperature profiles recorded during copolymerization reactions of different monomer compositions. **a** Variation of the amount of radical initiator (10% allyl glycigyl ether; 90% butyl acrylate). *Dashed line* 1.4%, *solid line* 1%, *thick solid line* 0.67%, *thick dashed line* 0.4% of azobisisobutyronitrile. **b** Variation of the monomer composition (initiator 1% azobisisobutyronitrile). *Dashed line* 5% allyl glycigyl ether and 95% butyl acrylate, *solid line* 10% allyl glycigyl ether and 90% butyl acrylate, *thick dashed line* 15% allyl glycigyl ether and 85% butyl acrylate, *thick solid line* 20% allyl glycigyl ether and 80% butyl acrylate

individual monomers and the monomer composition on the reproducibility of the polymerization reaction.

To demonstrate this, a series of experiments was performed in which the monomer mixture consisting of 9 ml of allyl glycigyl ether (10%) and butyl acrylate (90%) was passed through a column with different loading of an inhibitor remover. The reaction mixtures were immediately polymerized, and the temperature profile during polymerization was recorded (Fig. 7). The delay of polymerization is obviously highly dependent on the removal of the radical inhibitor with an exponential decrease, which is leveling off at a column length of about 20 cm (Fig. 7a). Moreover, different amounts of the same monomer mixture (11 to 20 ml) were passed through a 20-cm inhibitor remover column. The temperature profiles during subsequent copolymerization were found to be almost identical (Fig. 7b), which suggest that a column length of 20 cm is sufficient to remove the radical inhibitor.

To further improve the reproducibility of the copolymerization reaction, the effect of the duration of argon bubbling for removing of molecular oxygen on the delay of polymerization was investigated. The variation of the delay of polymerization was highly dependent on small fluctuations of the bubbling rate, which are caused by variations in the argon pressure in combination with the initial viscosity of the monomer mixture. Removal of oxygen by argon bubbling was hence considered to be rather a source for irreproducibility and was therefore not performed in the following experiments.

Another source of irreproducibility was seen in potential handling errors caused by manual preparation of the monomer mixtures. To exclude this, an automated liquid handling workstation (Tecan RSP 9000 equipped with XLP6000 pump) was adapted by means of an in-house programmed software module, which allows automated preparation of the monomer mixtures in a highly reproducible way. Up to eight reaction tubes can be filled with preprogrammed amounts of up to 20 different monomers. Operational parameters of the liquid handling workstation and the used syringe pump such as pump speed during aspiration and dispensing were optimized to increase accuracy and precision for the liquid transfer. Copolymerization was performed with the automatically prepared monomer mixtures, and the temperature profiles during

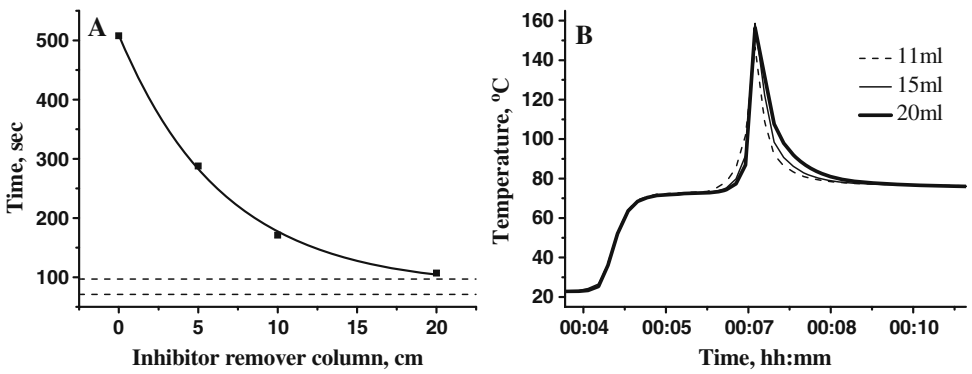

Fig. 7 Dependence of the delay of the polymerization derived from in situ recorded temperature profiles from the length of the inhibitor remover column (**a**). Temperature profiles for copolymerization reactions of different volumes of the same monomer mixture (10% allyl glycigyl ether, 90% butyl acrylate) after inhibitor removal by means of a 20-cm-long column (**b**)

copolymerization were compared with monomer mixtures, which were prepared by manual pipetting. The reproducibility of the copolymerization as derived from the temperature profiles during the reaction obtained with monomer mixtures prepared by manual versus robotic pipetting is compared in Table 2.

The overall heat during the copolymerization reactions derived from the integral of the temperature–time curve is independent from the pipetting process. However, variations in the maximum temperature during copolymerization are highly dependent on the accuracy of the preparation of the monomer mixture. Manual preparation exhibits a slightly better accuracy than robotic preparation using the 1,000-µl syringe. On the other hand, despite the improved reproducibility in the case of automatic pipetting using the 100-µl syringe, the pipetting time is very long. The time needed for the preparation of eight monomer mixtures with a volume of 3 ml using robotic pipetting with the 100-µl syringe is about 3 h as compared to about 20 to 25 min for both the manual as well as the robotic pipetting using the 1,000-µl syringe. However, this may be easily overcome by integration of a second syringe pump into the robotic pipetting system, allowing to choose the optimal syringe size depending on the overall pipetting volume and the necessary accuracy.

Using the automatic pipetting system, removal of the polymerization inhibitor and the described parallel synthesizer with improved stirring and temperature control is the basis for a reproducible synthesis of electrodeposition polymer libraries. In addition, the preparation of related biosensors has to be performed in a highly reproducible way to allow to compare the impact of the different electrodeposition polymers from a library on the biosensor properties. This is a prerequisite for the envisaged rational design of optimal electrodeposition polymers with specifically adapted properties.

A previously developed electrochemical robotic system [40] was further adapted for automatic biosensor fabrication, avoiding any manual preparation steps. The electrochemical robotic consists of a step-motor driven *x*,*y*-table as basis for a 96-well microtiter plate (Fig. 8).

Table 2 Comparison of the reproducibility of the copolymerization reaction in dependence from manual and robotic modes for preparation of monomer mixtures

	Temperature profiles		Operation time, min
	T_{max}, SD in %	Area, SD in %	
Manual	7.7	6.8	25
Robotic 1,000 µl	9.6	6.2	21
Robotic 100 µl	1.9	6.3	187

The syringe volume of the syringe pump for automatic pipetting can be adjusted to either 100 or 1,000 µl total volume

Using a glass plate on top of a Teflon lid, the humidity and hence the solvent evaporation as well as the atmosphere (e.g., inert gas) can be controlled. An electrode bundle consisting of a Pt working electrode, a Pt counter electrode, a miniaturized Ag/AgCl reference electrode, and if needed a capillary for the addition of solutions are moved through a hole in the glass plate into a well of the microtiter plate or alternatively into the glass vials positioned outside of the microtiter plate. After positioning of the electrodes, a variety of electroanalytical techniques such as cyclic voltammetry, chronoamperometry, and differential pulse voltammetry can be performed. In addition, the electrode bundle can be moved in *z*-direction for stirring, compounds can be added at predefined times using a step-motor driven syringe pump, and the working electrode can be dipped into a solution for electrode modification by dip coating. The in-house-developed software is highly modular using an easy-to-use script language predefining complex electroanalytical sequences.

To improve the reproducibility of automatic biosensor fabrication and testing using the electrochemical robotic system, some additional features had to be implemented, and electroanalytical sequences had to be evaluated and optimized. In a conventional biosensor calibration procedure using chronoamperometry, aliquots of the analyte are added to the electrolyte solution, and the current response of the sensor is recorded over time. For this, it is essential that the analyte is immediately homogeneously mixed in the electrolyte solution, which can be usually achieved by stirring. Initially it was assumed that due to the small electrolyte volume in the well of the microtiter plate, stirring can be avoided, and homogeneous distribution of the analyte is achieved fast. In Fig. 9, two biosensor calibration methods are compared. Figure 9a shows a chronoamperometric measurement in which glucose stock solution was repeatedly added into a well of the microtiterplate in which the biosensor was previously placed. A nearly continuous increase of the current has been recorded if the glucose solution was dispensed into the well using the syringe pump of the robotic system while the microtiter plate shaker was switched on (black line in Fig. 9a). Despite its difficult handling, the use of small magnetic stirring bars in the microtiter plate wells led to a significant improvement (gray line in Fig. 9a). Moving the electrode bundle into one of the vials at the external positions, which was filled with a glucose solution of known concentration (Fig. 9b), led to reliable chronoamperometric measurements. By using a digital I/O card, it was possible to switch on the potentiostat only after the electrode bundle was placed into the electrolyte, thus avoiding unwanted potential overswinging. As a matter of fact, after dipping the

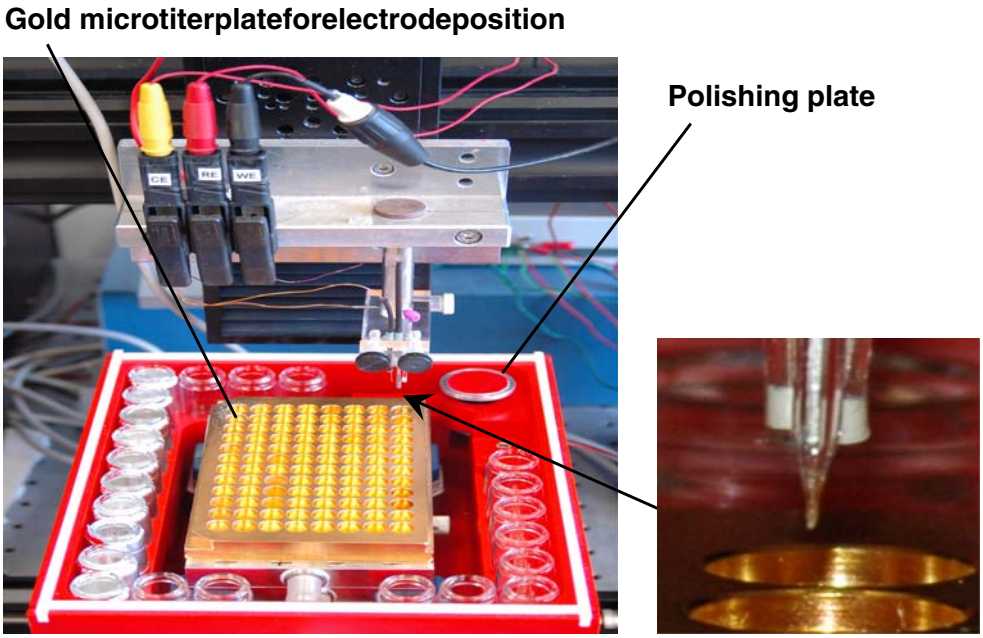

Fig. 8 Photograph of the electrochemical robotic system showing a 96-well gold microtiter plate in a chamber for controlling the atmosphere. For this, the chamber is covered by a glass plate and may be flushed with a humidified inert gas. The microtiter plate is placed on top of a shaking unit, and the whole chamber can be moved using a step-motor controlled *x*,*y*-positioning unit. The electrode holder is moved in the *z*-direction, and the electrodes are lowered into the wells through a hole in the glass plate. The electrodes can be additionally moved into the glass vials at the external positions for cleaning or calibration. In addition, the working electrode can be automatically repolished on the polishing wheel

electrode bundle into the glucose-containing electrolyte solution, a decay of the onset current was seen, which leveled off after a waiting time of about 60 s. Thus, current values at times higher than 60 s were used for construction of the calibration curves.

Another significant improvement of the reproducibility of the automatic biosensor fabrication and its evaluation is connected with the separation of pulse deposition of the electrodeposition polymer under simultaneous entrapment of the enzyme and sensor evaluation. Earlier, the same reference and counter electrodes were used during sensor fabrication and sensor evaluation. As a matter of fact, the counter and reference electrode were contaminated with adsorbed electrodeposition polymer, causing an unpredictable and not reproducible amount of enzyme activity being adsorbed on all surfaces, which were in contact with the polymer/enzyme solution. To overcome this problem, it had to be assured that the counter and reference electrode, which were used during the sensor evaluation, did not dip into the electrodeposition solution. For this, both the counter and the reference electrode of the electrode bundle were retracted (see Fig. 8) and thus exclusively used during sensor evaluation. Due to the precise control of the *z*-position of the electrode bundle with a nominal resolution of about 1 μm, any contact of the counter and reference electrode with the enzyme/polymer solution could be avoided. For the electrochemically induced precipitation of the electrodeposition polymer, a Au microtiter plate (see Fig. 8) was designed, which was connected as counter electrode during sensor fabrication. This leads to a defined relative position of the sensor electrode and the large counter

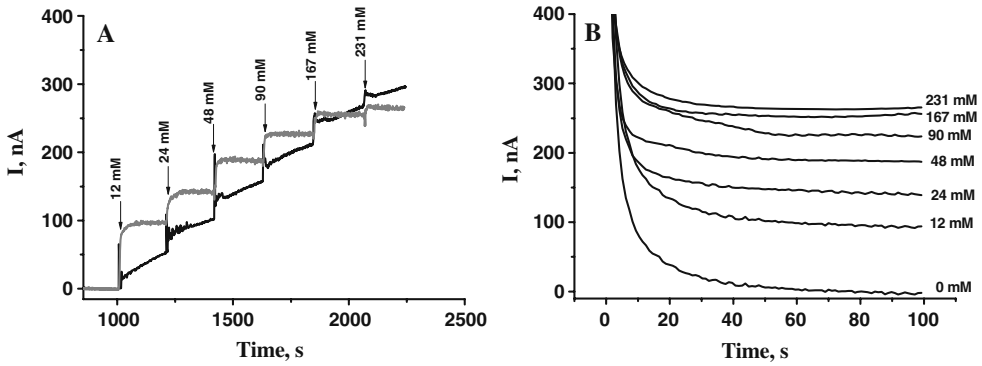

Fig. 9 Chronoamperometric biosensor calibration using the robotic system (platinized graphite electrode d=0.5 mm). **a** *Gray line* permanent stirring with magnetic stirring bars, *black line* mixing with the microtiter plate shaker. **b** Dipping of the biosensor into vials at external positions outside of the coordinates of the microtiter plate, which contained known concentrations of glucose solutions. The biosensor was connected to the potentiostat using a relay switch after the electrode bundle was placed in the electrolyte solution

electrode, thus assuring a reproducible establishment of the pH modulation during sensor preparation.

Besides characterization of the bare electrode surface prior to the polymer deposition, sensor formation and automatic recording of calibration plots, one major problem is the reliable cleaning of the electrode surface and the quantitative removal of the deposited polymer film. In earlier work [40], it was shown that electrochemical cleaning of the electrodes in 5 M HCl at a constant potential of 3 V versus Ag/AgCl/3 M KCl was possible, assuming that the cleaning is caused by the formed Cl_2. However, less attention was paid to the conditioning of the electrode surface by this aggressive cleaning protocol. Using the electrochemical robotic system, it is straightforward to use cyclic voltammetry in the presence of a well-known free-diffusing redox mediator such as 5 mM $[Ru(NH_3)_6]^{2+/3+}$ to monitor the quality of the electrode surface after cleaning.

In Fig. 10, a series of cyclic voltammograms is depicted, showing the voltammograms of the bare electrode surface before the electrochemically induced polymer precipitation, of the polymer-modified electrode, and of the electrode after cleaning by electrochemical formation of Cl_2. The current decrease in the case of the polymer-modified electrode clearly proves the successful modification of the electrode with the electrodeposition polymer, causing the observed hindered diffusional access of the $[Ru(NH_3)_6]^{2+/3+}$ to the electrode surface. In Fig. 10a, it becomes obvious that—despite the successful removal of the polymer film by the oxidative treatment with the in situ formed Cl_2—the cleaning procedure leads to a significant increase in the active electrode surface as compared with the initial bare electrode. In order to avoid the harsh conditions during Cl_2 formation, a polishing wheel was integrated within the electrochemical robotic system (see Fig. 8). The rotation of the polishing wheel can be switched on and off during the course of the analytical sequence, and the precision of the *z*-positioning enables the secure approach of the electrode to the surface of the polishing cloth. Cleaning by polishing re-established the initial electrode surface (Fig. 10b) and hence contributed significantly to a reproducible automated sensor fabrication and testing.

Finally, 16 different electrodeposition polymers were synthesized by emulsion polymerization at a temperature of 100 °C using azobisisobutyronitrile (AIBN) as radical initiator (Table 3). The obtained copolymers were neutralized with the corresponding amount of 10 M HCl, dissolved in about 20 ml methanol, which was then slowly replaced by water at 80 °C. Stable polymer suspensions with a solid content of about 20% were obtained. Aliquots of the emulsions of the electrodeposition polymers were weighed and precipitated with 10 M KOH. After washing with water, the precipitated polymers were dried at 120 °C for 30 min, reweighed, and then redissolved in methanol-d_4. The copolymer compositions were derived by regression analysis of the corresponding ^{1}H NMR spectra (Table 4). For this, the ^{1}H NMR spectra were divided into six regions corresponding to protons of different functionality. The composition of the copolymer was derived by the combination of the integrals of the peaks in the theoretically expected NMR spectra of a polymer. Biosensor fabrication and evaluation was performed automatically in the electrochemical robotic system. For this, the electrode was cleaned by polishing on the integrated polishing wheel, characterized by cyclic voltammetry in 5 mM $[Ru(NH_3)_6]^{2+/3+}$, and positioned in a well of the Au microtiter plate containing a mixture of an electro-

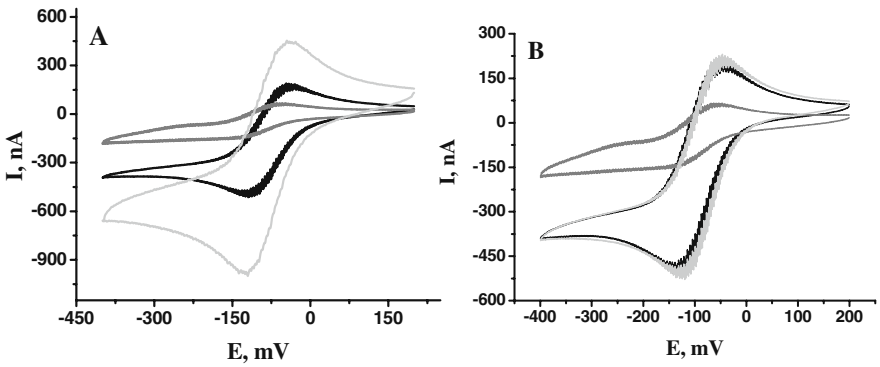

Fig. 10 Cyclic voltammograms from a three-electrode bundle as used for sensor preparation in the electrochemical robotic system (working electrode, 250 µm Pt disk; counter electrode, Pt; reference electrode, Ag/AgCl 3 M KCl) obtained in 5 mM $[Ru(NH_3)_6]Cl_3$ in the presence of 100 mM KCl as supporting electrolyte (sweep rate 50 mV/s). The cyclic voltammograms were recorded before the electrochemical-induced precipitation of an electrodeposition polymer (*black line*), of the polymer-modified electrode (*gray line*), and after the cleaning process (*light-gray line*). **a** Cleaning was performed electrochemically in 5 M HCl by applying a constant potential of 3 V versus Ag/AgCl/3 M KCl for 6 min. **b** Cleaning was performed mechanically on the polishing wheel integrated within the robotic system

Table 3 Monomer composition of the members of the cathodic electrodeposition polymer library

Monomers mixture	Styrene (%)	Butyl acrylate (%)	Dimethylaminoethyl methacrylate (%)	2-Hydroxyethyl methacrylate (%)
P1	7.19	50.98	34.64	7.19
P2	45.50	5.21	1.90	47.39
P3	13.57	28.53	27.15	30.75
P4	23.05	14.70	33.72	28.53
P5	18.04	11.37	28.63	41.96
P6	23.64	38.34	30.03	7.99
P7	20.21	38.34	1.55	39.90
P8	18.36	42.97	36.33	2.34
P9	15.95	48.64	30.74	4.67
P10	26.81	35.32	29.79	8.09
P11	40.13	16.83	12.30	30.74
P12	17.73	39.13	10.03	33.11
P13	–	15.57	77.87	6.56
P14	4.47	36.87	29.05	29.61
P15	30.94	20.14	35.25	13.67
P16	9.40	48.72	41.88	–

The relative composition of styrene, butyl acrylate, dimethylaminoethyl methacrylate, and 2-hydroxyethyl methacrylate was varied in the reaction volume by means of automatic pipetting

deposition polymer with glucose oxidase. The insertion depth of the working electrode was adjusted to make sure that the reference and counter electrode of the electrode bundle were not contaminated with the polymer/enzyme mixture. After electrochemical-induced polymer precipitation and entrapment of the enzyme within the precipitating polymer film, the as-prepared sensor was rinsed in phosphate buffer pH 6.3 and subsequently sequentially positioned in the glass vials placed at the external positions of the robotic system. The glass vials were filled with increasing concentrations of glucose in buffer of pH 6.3.

Table 4 Polymer composition of the members of the cathodic electrodeposition polymer library derived from the corresponding NMR spectra

Polymer	Styrene (%)	Butyl acrylate (%)	Dimethylaminoethyl methacrylate (%)	2-Hydroxyethyl methacrylate (%)
P1	8	46	40	6
P2	43	0	5	52
P3	14	23	24	39
P4	23	3	35	39
P5	19	6	27	48
P6	26	33	33	8
P7	21	33	6	40
P8	25	28	38	9
P9	19	51	30	0
P10	30	30	32	8
P11	42	6	16	36
P12	16	42	12	30
P13	0	25	65	10
P14	4	31	32	34
P15	32	26	32	10
P16	10	46	44	0

After inserting the electrode bundle into the glucose solution, the sensor electrode was connected to the working electrode connector at the potentiostat by means of a relay switch. By this, the working potential of +600 mV was applied to the sensor electrode, leading to the oxidation of enzymatically produced H_2O_2 and hence to a glucose-proportional current. The current was recorded for a predefined time (e.g., 120 s) before the electrode bundle was moved to the next higher glucose concentration. The current values after 60 s were used for the construction of the calibration graphs from which the apparent maximal current and the apparent Michaelis constant were derived (Fig. 11).

In general, all sensors show a comparatively small variation in K_M^{app}, which is mainly governed by the polymer film thickness as well as the diffusion and partitioning of the substrate glucose within the polymer/enzyme network. The I_{max}^{app} shows significant variations of a factor of up to 10. Obviously, sensors based on polymer P7 are best with respect to signal height, while P12 seems to be superior in terms of increased linear range with still sufficient sensitivity.

The preparation of libraries of electrodeposition polymers using a controlled and reproducible synthesis procedure together with an automatic sensor fabrication protocol employing an electrochemical robotic system is a prerequisite for finally elucidating the specific impact of the polymer composition, film thickness, enzyme-to-

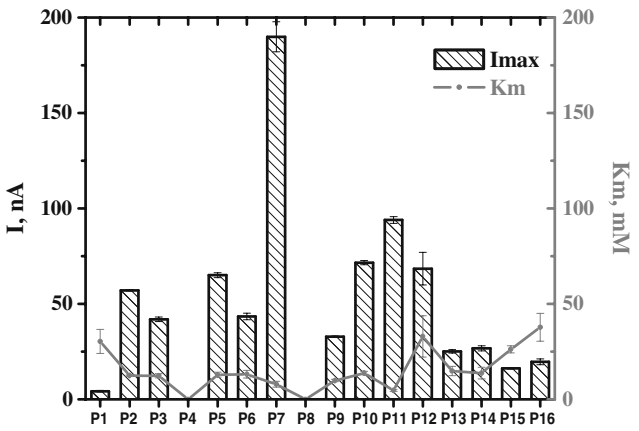

Fig. 11 K_M^{app} and I_{max}^{app} values of amperometric glucose biosensors obtained from 16 different cathodic electrodeposition paints (250 μm Pt electrode: potential pulse profile for electrodeposition, −1.2 V/0.2 s and 0 V/5 s; 100 mM phosphate buffer pH 6.3)

polymer ratio, etc., on the biosensor response. This evaluation is only possible if the detected variations in sensor response are not masked by irreproducibility in any of the steps from synthesis to biosensor fabrication.

Conclusion

The reproducible synthesis of libraries of electrodeposition polymers in small volumes and in a parallel process involving the combinatorial mixing of a large number of monomers was addressed by analysis of the reaction products and by improving instrumentation and in-line control of the temperature during polymerization. By removing polymerization inhibitors, accurate pipetting of the monomer mixtures using a specifically adapted pipetting robot and recording of the temperature in each reaction tube during polymerization the polymer synthesis can be controlled to achieve a sufficient degree in reproducibility. Simple bulk polymerization was found to be difficult to control due to the highly exothermic polymerization reaction and changes in viscosity which make temperature control in small volumes difficult. Polymerization in solution or emulsion overcomes many of the disadvantages of bulk polymerization such as thermal and viscosity problems. On the other hand, the presence of a solvent or a dispersing medium causes new challenges like chain transfer to the solvent and a shift from the composition of the monomer mixture and resulting copolymer.

In addition, the properties of an electrochemical robotic system were extended to improve the reproducibility of automatic sensor fabrication and evaluation. Integration of a Au microtiter plate used as counter electrode, a polishing wheel for electrode cleaning, and avoiding the contamination of the counter and reference electrode by the polymer/enzyme mixture were shown to allow a reproducible sensor fabrication and the comparison of the impact of the polymer composition on the properties of the derived biosensors.

Experimental part

Materials

Allyl glycigyl ether (97%), AIBN (99%), *n*-butyl acrylate (BA, 98%), 2-hydroxyethyl methacrylate (99%), *tert*- butylhydroperoxide, triethylamine (99%), and styrene (St, 99%) were purchased from Fluka (Buchs, CH). 2-Pyridinecarboxyaldehyde (99%) and glyoxal (40% solution in water) were obtained from Acros (Geel, Belgium). Methyl-4-imidazolecarboxylate (98%), 4-pyridinpropanol (96%), 1-(2-hydroxyethyl)imidazole (95%), and sodium hydride (95%) were obtained from Aldrich (Taufkirchen, Germany). Methacryloyl chloride (96%) and glucose oxidase (EC 1.1.3.4, type XS, 100,000–250,000 units/g of solid, from *Aspergillus niger*) were obtained from Sigma-Aldrich Chemie (Steinheim, Germany). Benzene, isopropanol, glucose, ethanol (abs), methanol, chloroform, ammonium hydroxide (25%), sodium carbonate, sodium hydrogen phosphate, potassium hydroxide, and hydrochloric acid (37%) were purchased from J.T. Baker (Deventer, Netherlands). Potassium dihydrogenphosphate was purchased from VWR International (Darmstadt, Germany). 2-Chloroethanol (99%) and sodium sulfate were obtained from Riedel-de-Haen (Seelze, Germany). 2-(Dimethylamino)ethylmethacrylate (DMAEMA, 98%) was purchased from Merck (Darmstadt, Germany). (2-Chloroethoxy)ethanol and 2- (2-chloroethoxy)-ethoxy ethanol were obtained from ABCR (Karlsruhe, Germany). *N*, *N*-Dimethyl-2,2-bis- imidazole and (2-pyridyl)imidazole were synthesized according to literature [41, 42].

Instrumentation and equipment

For preparation of monomer mixtures, either a specifically adapted automated liquid handling workstation Tecan RSP 9000 equipped with a XLP6000 pump in robotic mode (Tecan Deutschland, Crailsheim, Germany) or a set of Eppendorf dispensers (variable volume 10–100 µl; 100–1,000 µl; Eppendorf, Hamburg, Germany) was used. The workstation and pump were controlled by in-house-written software (VBA in Microsoft Excel).

Parallel polymerization was carried out in a newly designed polymerization block equipped with a RCT basic IKAMAG safety control heating plate connected to an IKA ETS-D6 contact thermometer (IKA, Staufen, Germany). A digital overhead stirrer (IKA EUROSTAR power control-visc., IKA, Staufen, Germany) with integrated rotation-speed control was connected to up to eight stirring bars with integrated thermocouples (type "T", Conatex, Sankt Wendel, Germany) connected to a Plug-In USB-5201 datalogger (PLUG-IN Electronic, Eichenau, Germany) for continuous readout of the temperature from all reaction tubes.

^{1}H NMR and ^{13}C NMR spectra were recorded with a Bruker DRX 400 spectrometer in methanol-d_4 (Deutero, Kastellaun, Germany); chemical shifts in ppm (δ) were referenced to the residual solvent signal. NMR data were evaluated using the MestRec Lite v 4.59 software (MestRec, Santiago de Compostela, Spain).

Graphite rods (type RW001, 3.05 or 0.5 mm diameter) from Ringsdorff Werke (Bonn, Germany), sealed in glass tubes by means of epoxy glue and used as working electrodes, were polished with emery paper of decreasing size and rinsed with 20 mM phosphate buffer pH 6.3. Pt electrodes (d=250 µm) were fabricated in house. Manual

amperometric measurements at constant potential were performed with an Autolab system (Eco Chemie, Utrecht, The Netherlands). An in-house built electrochemical robotic system was used for automatic fabrication and evaluation of glucose biosensors.

Synthesis of acrylate-based monomers

The functionalized alcohol was dissolved in $CHCl_3$ or CH_2Cl_2, and the corresponding amount of triethylamine was slowly added. The mixture was cooled to 0 °C. Methacryloyl/acryloyl chloride (5% excess) in $CHCl_3$ was added dropwise under continuous stirring at 2–3 °C. The reaction mixture was kept at this temperature for 1 h and then stirred for another 10 h at RT. The reaction mixture was washed with saturated Na_2CO_3 solution and three times with water and dried over Na_2SO_4, and the solvent was evaporated under vacuum. The molecular structures of the obtained monomers were confirmed by means of GC-MS and NMR.

Polymer synthesis

Before polymerization, the monomers were passed through an inhibitor remover column (Sigma-Aldrich Chemie, Steinheim, Germany).

Emulsion polymerization with electrostatic stabilization (1) was carried out as described previously [17, 20, 24]. As radical initiator *tert*-butyl-hydroperoxide was added to the mixture of the monomers, which was neutralized with the corresponding amount of 3 M HCl. The copolymerization was initiated by heating the mixture in a specifically designed reaction tube with a reflux condenser to a temperature of 90 °C for 5 h. The obtained copolymer was dissolved in a minimal amount of methanol.

Emulsion polymerization (2) was performed by the addition of the radical initiator (10% AIBN in benzene) to the emulsion of the monomers in 2 ml water. The copolymerization was initiated by heating the mixture in a specifically designed reaction tube with a reflux condenser to a temperature of 70 °C. The obtained copolymer was neutralized with the corresponding amount of 10 M HCl and diluted with 3 ml methanol.

Bulk polymerization was done by the addition of the radical initiator (10% AIBN in benzene) to the mixture of the monomers. The copolymerization was initiated by heating the mixture in a specifically designed reaction tube with a reflux condenser to a temperature of 70 °C for 5 h. The obtained copolymer was neutralized with a corresponding amount of 10 M HCl and dissolved in 5 ml methanol.

Solution polymerization was done similar to the emulsion polymerization; however, water was replaced by methanol for readily dissolving the monomers.

The radical initiator (10% AIBN in benzene) was added to the solution of the monomers in 2 ml methanol. Then copolymerization was initiated by heating the mixture in a specifically designed reaction tube with a reflux condenser to a temperature of 70 °C for 5 h. The obtained copolymer was neutralized with the corresponding amount of 10 M HCl and diluted with 3 ml methanol.

Polymer characterization

The overall conversion of the reaction was determined by gravimetry. Samples of the electrodeposition polymers were weighed, dried at 120 °C for 30 min, reweighed, and then dissolved in methanol-d_4. The copolymer composition was derived by regression analysis from the ^{1}H NMR spectra.

Fabrication and characterization of amperometric biosensors

Manual sensor fabrication was done following a scheme previously described [16]. Pt-disk working electrodes were cleaned by polishing on a polishing cloth with alumina polishing paste (3, 1, and 0.3 μm) from Leco (Kirchheim, Germany). All electrochemical experiments were carried out at room temperature, and all potentials are referred versus a Ag/AgCl/3 M KCl reference electrode. The sequence for the automated biosensor screening protocol consists of the following steps: (1) electrode characterization by cyclic voltammetry in a solution of 5 mM $[Ru(NH_3)_6]^{2+/3+}$, (2) washing in water, (3) precipitation of the polymer/enzyme film by means of a potentiostatic pulse profile (−1.2 V/0.2 s and 0 V/5 s, 20 pulses) in a gold microtiter plate, (4) washing of the modified electrode in 20 mM phosphate buffer (pH 6.3) and drying in air for 5 min, (5) swelling of the polymer film in 100 mM phosphate buffer (pH 6.3), (6) calibration of the biosensors by dipping of the glucose biosensor into the glucose solutions of known concentrations at an applied potential of 600 mV, (7) washing in water, and (8) polishing of the electrode on the polishing plate.

Acknowledgments H. Shkil is grateful for the financial support from the German Academic Exchange Service (DAAD) for a PhD fellowship. The authors are grateful to Armin Lindner and his colleagues from the mechanical workshop for continuous support during the instrumental development and to the European Commission for financial support in the framework of the project 3D-NANOBIODEVICE (NMP4-SL-2009-229255).

References

1. Yang X, Johansson G, Gorton L (1989) A glucose sensor made by chemically crosslinking glucose oxidase directly on the surface of a carbon electrode modified with Pd/Au for hydrogen peroxide electrocatalysis. Microchim Acta 97:9–16

2. Künzelmann U, Böttcher H (1997) Biosensor properties of glucose oxidase immobilized within SiO_2 gels. Sens Actuators B 39:222–228
3. Wang B, Li B, Deng Q, Dong S (1998) Amperometric glucose biosensor based on sol–gel organic–inorganic hybrid material. Anal Chem 70:3170–3174
4. Nagata R, Yokoyama K, Clark SA, Karube I (1995) A glucose sensor fabricated by the screen printing technique. Biosens Bioelectron 10:261–267
5. Rohm I, Kuennecke W, Bilitewski U (1995) UV-polymerizable screen-printed enzyme pastes. Anal Chem 67:2304–2307
6. Gernet S, Koudelka M, de Rooij NF (1989) A planar glucose enzyme electrode. Sens Actuators 17:537–540
7. Newman JD, Turner APF, Marrazza G (1992) Ink-jet printing for the fabrication of amperometric glucose biosensors. Anal Chim Acta 262:13–17
8. Johnson KW (1991) Reproducible electrodeposition of biomolecules for the fabrication of miniature electroenzymatic biosensors. Sens Actuators B 5:85–89
9. Strike DJ, de Rooij NF, Koudelka-Hep M (1995) Electrochemical techniques for the modification of microelectrodes. Biosens Bioelectron 10:61–66
10. Barlett PN, Cooper JM (1993) A review of the immobilization of enzymes in electropolymerized films. J Electroanal Chem 362:1–12
11. Schuhmann W (1995) Conducting polymer based amperometric enzyme electrodes. Microchim Acta 121:1–29
12. Cosnier S (1999) Biomolecule immobilization on electrode surfaces by entrapment or attachment to electrochemically polymerized films. A review. Biosens Bioelectron 14:443–456
13. Gerard M, Chaubey A, Malhotra BD (2002) Application of conducting polymers to biosensors. Biosens Bioelectron 17:345–359
14. Habermüller K, Ramanavicius A, Laurinavicius V, Schuhmann W (2000) An oxygen-insensitive reagentless glucose biosensor based on osmium-complex modified polypyrrole. Electroanalysis 12:1383–1389
15. Reiter S, Habermüller K, Schuhmann W (2001) A reagentless glucose biosensor based on glucose oxidase entrapped into osmium-complex modified polypyrrole films. Sens Actuators B 79:150–156
16. Kurzawa C, Hengstenberg A, Schuhmann W (2002) Immobilization method for the preparation of biosensors based on pH shift-induced deposition of biomolecule-containing polymer films. Anal Chem 15:355–361
17. Neugebauer S, Isik S, Schulte A, Schuhmann W (2003) Acrylic acid-based copolymers as immobilization matrix for amperometric Biosensors. Anal Lett 36:2005–2020
18. Beck F (1976) Fundamental aspects of electrodeposition of paint. Prog Org Coat 4:1–60
19. Krylova I (2001) Painting by electrodeposition on the eve of the 21st century. Prog Org Coat 42:119–131
20. Ngounou B, Neugebauer S, Frodl A, Reiter S, Schuhmann W (2004) Combinatorial synthesis of a library of acrylic acid-based polymers and their evaluation as immobilisation matrix for amperometric biosensors. Electrochim Acta 49:3855–3863
21. Kueng A, Kranz C, Mizaikoff B (2004) Amperometric ATP biosensor based on polymer entrapped enzymes. Biosens Bioelectron 19:1301–1307
22. Shkotova LV, Goriushkina TB, Tran-Minh C, Chovelon J, Soldatkin AP, Dzyadevych SV (2008) Amperometric biosensor for lactate analysis in wine and must during fermentation. Mater Sci Eng C 28:943–948
23. Shkotova LV, Soldatkin AP, Gonchar MV, Schuhmann W, Dzyadevych SV (2006) Amperometric biosensor for ethanol detection based on alcohol oxidase immobilised within electrochemically deposited Resydrol film. Mater Sci Eng C 26:411–414
24. Ngounou B, Aliyev EH, Guschin DA, Sultanov YM, Efendiev AA, Schuhmann W (2007) Parallel synthesis of libraries of anodic and cathodic functionalized electrodeposition paints as immobilization matrix for amperometric biosensors. Bioelectrochemistry 71:81–90
25. Mayo FR, Lewis FM (1944) Copolymerization. I. A basis for comparing the behavior of monomers in copolymerization; the copolymerization of styrene and methyl methacrylate. JACS 66:1594–1601
26. Alfrey T Jr, Goldfinger G (1944) The mechanism of copolymerization. J Chem Phys 12:205–209
27. Greenley RZ (1999) In: Brandrup J, Immergut EH, Grulke EA (eds) Polymer handbook, 4th edn. Wiley, New York, pp 81–320
28. Doiuchi T, Minoura Y (1977) Asymmetric induction by interfacial emulsion copolymerization of styrene with maleic acid in the presence of lecithin. Macromolecules 10:260–265
29. Plochocka K (1981) Effect of the reaction mediumon radical copolymerization. J Macromol Sci Rev Macromol Chem Phys C20:67–148
30. Ponratnam S, Kapur SK (1977) Reactivity ratios of ionizing monomers in aqueous-solution—copolymerization of acrylic and methacrylic acids with acrylamide. Macromol Chem Phys 178:1029–1038
31. Truong ND, Galin JC, Francois J, Pham QT (1986) Microstructure of acrylamide acrylic-acid copolymers. 1 as obtained by alkaline-hydrolysis. Polymer 27:459–466
32. Madruga EL (2002) From classical to living/controlled statistical free-radical copolymerization. Prog Polym Sci 27:1879–1924
33. Venkatesh R, Vergouwen F, Klumperman B (2004) Copolymerization of allyl butyl ether with acrylates via controlled radical polymerization. J Polym Sci, Part A: Polym Chem 42:3271–3284
34. Gu B, Liu S, Leber JD, Sen A (2004) Nitroxide-mediated copolymerization of methyl acrylate with 1-alkenes and norbornenes. Macromolecules 37:5142–5144
35. Liu S, Gu B, Rowlands HA, Sen A (2004) Controlled random and alternating copolymerization of methyl acrylate with 1-alkenes. Macromolecules 37:7924–7929
36. Venkatesh R, Harrisson S, Haddleton DM, Klumperman B (2004) Olefin copolymerization via controlled radical polymerization: copolymerization of acrylate and 1-octene. Macromolecules 37:4406–4416
37. Bevington JC, Huckerby TN, Hunt BJ, Jenkins AD (2001) Further study of allyl ethers and related compounds as transfer agents in radical polymerizations. J Macromol Sci Part A Pure Appl Chem 38:981–990
38. Hadjikallis G, Hadjiyannakou SC, Vamvakaki M, Patrickios CS (2002) Synthesis and aqueous solution characterization of novel diblock polyampholytes containing imidazole. Polymer 43:7269–7273
39. Cui L, Lattermann G (2002) Synthesis and characterization of new acrylate and methacrylate monomers with pendant pyridine groups. Macromol Chem Phys 203:2432–2437
40. Reiter S, Ruhlig D, Ngounou B, Neugebauer S, Janiak S, Vilkanauskyte A, Erichsen T, Schuhmann W (2004) An electrochemical robotic system for the optimization of amperometric glucose biosensors based on a library of cathodic electrodeposition paints. Macromol Rapid Commun 25:348–354
41. Liu FJ, Kokorudz JS, Collier HL (1988) Synthesis and characterization of urethane polymers containing 2, 2'-biimidazole. J Polym Sci, Part A: Polym Chem 26:3015–3029
42. Yue S, Xu H, Ma J, Su J, Kann Y, Zhang H (2006) Design and syntheses of blue lumenistent zinc(II) and cadmium(II) complexes with bidentate or tridentate pyridyl-imidazole ligands. Polyhedron 25:635–664